Regulatory Toxicology and Pharmacology 109 (2019) 104497

Contents lists available at ScienceDirect

Regulatory Toxicology and Pharmacology

journal homepage: www.elsevier.com/locate/yrtph

Comparison of metabolic and mitogenic response *in vitro* of the rapid-acting insulin lispro product SAR342434, and US- and EU-approved Humalog®

Marcus Korn[a,1], Paulus Wohlfart[a,*,1], Thomas Gossas[b], Mari Kullman-Magnusson[b], Birgit Niederhaus[a], Juergen Dedio[a], Norbert Tennagels[a]

[a] Sanofi-Aventis Deutschland GmbH, Industriepark Höchst, 65926, Frankfurt am Main, Germany
[b] Beactica AB, Virdings allé 2, 754 50, Uppsala, Sweden

ARTICLE INFO

Keywords:
Adipocyte lipolysis
Hepatocyte glucose-6-phosphatase gene expression
Insulin-like growth factor receptor-1
Insulin lispro
Insulin receptor
L6 myocyte glucose uptake
MCF-7 cell proliferation
Receptor binding/autophosphorylation
SAR342434
Surface plasmon resonance

ABSTRACT

SAR342434 is a biosimilar of insulin lispro (Humalog® U-100). Batches of SAR342434 were compared with Humalog® batches of either EU or US origin in a panel of *in vitro* biological assays that included insulin binding to insulin receptor (IR) isoforms A (IR-A) and B (IR-B) and IR-A/IR-B autophosphorylation. A surface plasmon resonance biosensor-based assay was developed to characterize the kinetics of insulin binding to solubilized full-length IR-A or IR-B. Insulin-dependent metabolic activity assays included inhibition of lipolysis in *in vitro* differentiated human adipocytes, glucose uptake in L6-myocytes, and repression of glucose-6-phosphatase gene expression in human hepatocytes. Mitogenic activity assays included insulin binding to insulin-like growth factor-1 receptor (IGF1R), IGF1R autophosphorylation, and cell proliferation in MCF-7 cells. Weighted geometric means and their respective 95% confidence intervals (CI) were calculated for all 50% inhibitory or effective concentration values and kinetic binding constants for IR-A and IR-B. Statistical evaluation of the data demonstrated that the 90% CIs of the ratio of geometric means between SAR342434 and Humalog® EU or Humalog® US were within the predefined acceptance limits for each assay. Insulin lispro as SAR342434 solution demonstrated similarity to both US- and EU-approved Humalog® based on a side-by-side biological similarity assessment.

1. Introduction

All patients with type 1 diabetes mellitus and some with type 2 diabetes mellitus require both a long-acting insulin, such as insulin glargine, to control fasting blood glucose levels, and a rapid-acting insulin to control prandial glucose levels. For many patients, use of rapid-acting insulin analogs with a prompt onset of action and a lower risk for hypoglycemia is recommended to control prandial glucose levels (American Diabetes Association, 2018).

Insulin lispro (Lys (B28), Pro (B29) human insulin), an analog of recombinant DNA origin, is the active ingredient of Humalog® products (Eli Lilly and Company, Indianapolis, IN, USA). This position swap of Lys (B28) and Pro (B29) does not alter insulin receptor (IR) binding but accelerates dissociation of insulin dimers and insulin hexamers after subcutaneous injection. As a result, this insulin analog has a more rapid onset of action than regular human insulin as more monomers are available for rapid absorption. Thus, insulin lispro is a rapid-acting insulin indicated to improve postprandial glycemic control in patients with diabetes mellitus.

SAR342434 (insulin lispro; Sanofi, Paris, France) has been developed as a biosimilar (follow-on) biological medicinal product to Humalog® U-100 in accordance with the relevant US and EU guidelines (US Food and Drug Administration and Center for Drug Evaluation and Research (CDER), 1999,US Food and Drug Administration and Center for Drug Evaluation and Research (CDER), 2008, European Medicines Agency, 2012,European Medicines Agency, 2014,European Medicines Agency, 2015). Protein-based therapeutics manufactured by distinct processes must be shown to be pharmacologically similar to be approved as biosimilar or follow-on products. Nonclinical studies should be comparative in nature and designed to demonstrate similarity of activity at the receptor level as well as similarity of biological activity (European Medicines Agency, 2015). For insulin biosimilars, a 2015 European Medicines Agency (EMA) guideline recommends an intensive, comparative characterization of the *in vitro* profile be undertaken before starting clinical development (European Medicines Agency, 2015).

* Corresponding author. Sanofi Aventis Deutschland GmbH, Industriepark Höchst, Building H821, 65926, Frankfurt am Main, Germany.
E-mail address: paulus.wohlfart@sanofi.com (P. Wohlfart).
[1] Both authors contributed equally to the publication.

https://doi.org/10.1016/j.yrtph.2019.104497
Received 22 May 2019; Received in revised form 25 September 2019; Accepted 7 October 2019
Available online 11 October 2019
0273-2300/

The *in vitro* profile should include receptor binding studies with both human insulin receptor isoforms (IR-A and IR-B), as well as metabolic and mitogenic response assays in comparison with the originator product. In addition to standard equilibrium binding studies, association/dissociation kinetics to the IR have to be determined (European Medicines Agency, 2015). Biological activity should be compared by both receptor autophosphorylation and metabolic activity assays. Earlier guidelines recommended at least two different assays be performed to confirm metabolic activity, while the latest guidelines recommend inclusion of at least a third different assay (European Medicines Agency, 2015). Binding to insulin-like growth factor-1 receptor (IGF1R) and a functional activity assay can also be included to cover potential mitogenic activity.

The aim of this study was to characterize the *in vitro* profile of different batches of SAR342434 compared with different batches of both US- and EU-marketed Humalog® in accordance with the latest EMA guidelines. In order to fulfill the approval guidelines, we developed a third robust metabolic cell assay, glucose-6-phosphatase expression in a new hepatocyte cell model. Furthermore, a new IR assay based on surface plasmon resonance and full-length IR isoforms A and B for the measurement of binding kinetics has been developed.

2. Materials and methods

SAR342434 was produced by recombinant DNA techniques, purified to homogeneity, and made available by Process Development Biotechnology (Sanofi-Aventis Deutschland GmbH, Frankfurt, Germany). Humalog® batches of US and EU origin were purchased from Phoenix Pharmahandel GmbH & CoKG (Mannheim, Germany) and Myoderm (Norristown, PA, USA). The batches of each insulin lispro product used in the studies are listed in Table 1. Human A14[^{125}I]-insulin was prepared by the radiosynthesis group of Sanofi-Aventis (Rissler and Engelmann, 1996). [2–^{14}C]-thymidine was obtained from PerkinElmer (Boston, MA, USA). Insulin-like growth factor-1 and -2 (IGF1, IGF2) were obtained from R&D Systems (Wiesbaden-Nordenstadt, Germany) and from Cell Sciences (Canton, MA, USA). Radiolabeled [125I]-IGF1 was ordered as custom radiosynthesis from ANAWA / Biotrend (Kloten, Switzerland). cOmplete™ Protease Inhibitor was from Roche (Penzberg, Germany). SPA PVT PEI treated WGA Beads were purchased from GE Healthcare (Amersham, UK). Cell culture reagents, biochemicals and antibodies were obtained from the suppliers as indicated in the individual assay sections or as described previously (Sommerfeld et al., 2010). All other chemicals were of reagent grade.

2.1. Insulin receptor kinetic binding

The kinetic binding of Humalog® EU, Humalog® US, and SAR342434 to human full-length IR-A and IR-B were analyzed by surface plasmon resonance (Subramanian et al., 2013). The experiments were performed using a Biacore™ T200 instrument and CM3 biosensor chips (GE Healthcare/Biacore, Uppsala, Sweden). An anti-IR alpha antibody (Abcam, Cambridge, UK, cat #36550, clone [83-7]) was covalently immobilized on the CM3 chips using standard amine coupling (GE Healthcare/Biacore). Plasma membranes were prepared from CHO cells overexpressing human IR-A or IR-B as previously described (see below and Sommerfeld et al., 2010). Human IR-A or IR-B membrane preparations were dissolved in 0.3 mL solubilization buffer (20 mM HEPES-NaOH buffer [pH 7.8]), 100 mM NaCl, 10 mM $MgCl_2$, 1% (w/v) n-Dodecyl-β-D-maltoside and freshly added cOmplete™ protease inhibitor tablets (Sigma-Aldrich, Stockholm, Sweden) and stored on ice for 60 min with occasional vortexing. Following centrifugation at 17,000 X g for 1 min, the supernatant containing solubilized IR was injected for 40 min over the antibody-coated surfaces. Concentration series of each insulin analog were prepared in 10 mM HEPES-NaOH buffer (pH 7.8), 150 mM NaCl, 0.05% Tween-20, and 10 mM $MgCl_2$, and each concentration was injected for 25 s at a flow rate of 30 µl/min. Each experiment was repeated on 5 different days with freshly captured IR. All experiments were performed at 25 °C.

Raw data sensorgrams were double referenced by subtraction of curves from the reference surface and blank injections, using Biacore™ T200 evaluation software V1.0 (GE Healthcare/Biacore). Data analysis was then performed by global regression analysis of whole sets of sensorgrams from a concentration series. Fitting efforts revealed a two-binding site interaction model with a high-affinity binding site and a low-affinity binding site, consistent with literature data (Subramanian et al., 2013). Overall, four kinetic constants were obtained: ka1 and kd1, the association and dissociation constants for the high-affinity binding site, and ka2 and kd2, the same constants for the low-affinity binding site.

Table 1
Insulin lispro products employed in this study.

Product	Batch No.	Batch Designation
SAR342434	C1033467	SAR342434-1
	5F006	SAR342434-2
	5F007	SAR342434-3
	5F008	SAR342434-4
Humalog® EU	C079720	Humalog EU-1
	C224081	Humalog EU-2
	C350360	Humalog EU-3
	C003027C	Humalog EU-4
Humalog® US	C018505C	Humalog US-1
	C152074A	Humalog US-2
	C257286C	Humalog US-3
	C087535A	Humalog US-4

2.2. Receptor competitive binding

The equilibrium binding of the different insulins to human IR-A, IR-B, or IGF1R was analyzed in a competitive binding assay using the scintillation proximity assay as previously described (Rissler and Engelmann, 1996). As a source of plasma membranes, Chinese Hamster Ovary cell lines (CHO) Flp-In (Invitrogen, Karlsruhe, Germany) was used, transfected with pcDNA5/FRT as an expression vector (Invitrogen, Karlsruhe, Germany, cat # V601020). Into pcDNA5/FRT either IR-A, or IR-B were cloned by standard technology. As starting point for IGF1R binding measurements, a mouse embryonic fibroblast (MEF) 3T3 Tet off cell line (BD Bioscience, Heidelberg, Germany, cat.# 630914) was transfected with a human IGF1R tetracycline-regulatable plasmid. Plasma membrane from these cell lines were prepared as described (Sommerfeld et al., 2010) and stored at −80 °C until use. All binding experiments were conducted in 96-well microplates. Briefly, per well membranes (2 µg total protein per well) were incubated with 0.25 mg WGA PVT PEI SPA beads, 100 pmol/L A14 [^{125}I]-insulin, and various concentrations of unlabelled insulins in a binding buffer containing 0.05 mol/L Tris-HCl (pH 7.8), 0.15 mol/L NaCl, 0.1% bovine serum albumin (BSA), and cOmplete™ Protease Inhibitor for 12 h at room temperature (23 °C). In case of IGF1R binding 100 pmol/L [125I]-IGF1 was used as tracer. The radioactivity was measured at equilibrium in a microplate scintillation counter (Wallac 1450 MicroBeta® TriLux scintillation counter; PerkinElmer, Freiburg, Germany). Human IGF1R binding experiments were conducted in a similar manner.

2.3. Receptor autophosphorylation

Chinese hamster ovary cells expressing human IR-A or IR-B were used for IR autophosphorylation assays using In-Cell Western technology as previously described (Sommerfeld et al., 2010). For the analysis of IGF1R autophosphorylation, the receptor was overexpressed in a mouse embryo fibroblast 3T3 Tet-Off Cell Line (BD Bioscience, Heidelberg, Germany) that was stably transfected with IGF1R

tetracycline-regulatable expression plasmid.

In order to determine the receptor tyrosine phosphorylation level, cells were seeded into 96-well plates and grown for 44 h. Cells were serum starved with serum-free Ham's F12 medium (Thermo Fisher Scientific, Dreieich, Germany), not supplemented with BSA, for 2 h. The cells were subsequently treated with increasing concentrations of either human insulin or the indicated insulin analog for 20 min at 37 °C. After incubation, the medium was discarded and the cells were fixed in 3.75% freshly prepared paraformaldehyde for 20 min. Cells were permeabilized with 0.1% Triton-X-100 in phosphate-buffered saline (PBS) for 20 min. Blocking was performed with Odyssey blocking buffer (LICOR, Bad Homburg, Germany) for 1 h at room temperature. Antiphosphotyrosine antibody 4G10 (Millipore, Schwalbach, Germany) was incubated for 2 h at room temperature. After incubation of the primary antibody, cells were washed with PBS + 0.1% Tween20. The secondary antimouse-immunoglobulin G-800-CW antibody (LICOR) was incubated for 1 h. Results were normalized by the quantification of DNA with TO-PRO-3 dye (Invitrogen, Karlsruhe, Germany). Data were obtained as relative units (RU) and are presented as fold over basal.

2.4. Inhibition of lipolysis

Insulin-mediated inhibition of lipolysis in *in vitro* differentiated human adipocytes has been described previously (Werner et al., 2014). Human preadipocytes from a subcutaneous depot were obtained in frozen aliquots from Cell Systems Biotechnologie Vertrieb GmbH (Troisdorf, Germany). For cell number expansion, the cells were cultured in Endothelial Cell Growth Medium supplemented with supplement mix (PromoCell GmbH, Heidelberg, Germany) at 37 °C in a humidified atmosphere. After the third passage, the expanded cell number was high enough to start the differentiation. For differentiation into adipocytes, detached and resuspended cells were seeded onto microtiter plates. After cell attachment, the cell medium was removed and replaced by differentiation medium (Dulbecco's Modified Eagle's Medium/Ham's F-10 Medium (1:1, volume per volume; PAN-Biotech GmbH, Aidenbach, Germany), 15 mM HEPES buffer (pH 7.4), 33 µM biotin, 17 µM pantothenate, 1 µM dexamethasone, 0.2 mM isobutylmethylxanthine, 10 nM L-thyroxine (all from Sigma-Aldrich Chemie GmbH, Taufkirchen, Germany), 3% (volume per volume) fetal calf serum (FCS; PAN-Biotech GmbH), 100 nM human insulin, 0.625 × Antibiotic-Antimycotin (Life Technologies GmbH, Darmstadt, Germany), 0.1 µM peroxisome proliferator-activated receptor gamma ($PPAR\gamma$) agonist.

After 3 days, the differentiation medium was replaced by adipocyte medium (as described above, but without isobutylmethylxanthine and L-thyroxine) and the plates were incubated for ≥ 10 additional days; the medium was changed on a 3-4-3–day cycle. Fourteen to 16 days after start of differentiation, the adipocyte medium was removed and replaced with adipocyte medium without insulin and $PPAR\gamma$ agonist. The plates were then incubated overnight at 37 °C. The next day the medium was removed, each well washed three times with lipolysis medium (medium 199, PAN-Biotech GmbH) supplemented with 1% (w/v) human free fatty acid free serum albumin (Sigma-Aldrich Chemie GmbH), and lipolysis medium containing the test insulins in dilution series added. The plates were incubated for 4 h at 37 °C in a humidified atmosphere, after which a defined volume of supernatant was removed from each well and analyzed for free glycerol content using the free glycerol determination kit (Sigma-Aldrich Chemie GmbH) according to the manufacturer's instructions.

2.5. Stimulation of glucose uptake

Creation of the L6-AS160_v2-GLUT4 cell line, cell culture conditions, and measurement of 2-deoxyglucose uptake have been described previously (Baus et al., 2010). L6-AS160_v2-GLUT4 cells were grown in Minimum Essential Medium alpha modification (MEMα; PAN-Biotech GmbH) supplemented with tetracycline-free 10% FCS (PAA Laboratories, Pasching, Austria), 2 µg/mL blasticidin (Life Technologies Corporation, Carlsbad, CA, USA), 0.5 µg/mL puromycin (Life Technologies Corporation), and 200 µg/mL hygromycin (Thermo Fisher Scientific). Expression of AS160_v2 protein was induced with 1 µg/mL doxycycline (Sigma-Aldrich Chemie). L6 wild-type cells were obtained from American Type Culture Collection (CRL1458) and grown in Gibco™ MEMα + GlutaMAX (Thermo Fisher Scientific) supplemented with tetracycline-free10% FCS (PAA Laboratories) and 1% penicillin/streptomycin (PAA Laboratories). L6- GLUT4-myc cells were grown in MEMα + GlutaMAX supplemented with tetracycline-free 10% FCS (PAA Laboratories), 1% penicillin/streptomycin (PAA Laboratories), and 2 µg/mL blasticidin (Thermo Fisher Scientific). All cells were grown at 37 °C and 5% CO_2.

L6-AS160_v2-GLUT4-myc cells were incubated in starvation medium (MEMα) 3–4 h prior to each experiment. For differentiation, the cells were grown in MEMα + GlutaMAX supplemented with 1% horse serum (Lonza Biochemicals, Portsmouth, NH, USA) for 7 days. Cells were plated in 96-well Cytostar-T scintillating microtiter plates. After 48 h, cells were serum starved (3–4 h) and treated with various concentrations of each insulin in serum-free buffer not supplemented with BSA. In detail, uptake of ^{14}C-labeled 2-deoxyglucose (0.01 MBq/well; GE Healthcare, Amersham, UK) was measured as described previously (Voss et al., 2005; Baus et al., 2008). Nonspecific uptake was determined in the presence of 40 µM cytochalasin B (Thermo Fisher Scientific) and subtracted from the total uptake. Radioactive counts were measured in a Wallac 1450 MicroBeta® TriLux scintillation counter (PerkinElmer, Shelton, CT, USA) as counts per min.

2.6. Repression of glucose-6-phosphatase gene expression

Frozen aliquots of Upcyte® human hepatocytes (Upcyte Technologies, Hamburg, Germany) were thawed and cells seeded in precoated collagen type-1 96-well plates (Greiner Bio-One, Kremsmünster, Austria) using Upcyte hepatocyte thawing medium and Upcyte hepatocyte insulin-free high-performance medium (containing supplement A and L-glutamine, respectively). The plates were incubated for 48h at 37 °C in a humidified atmosphere containing 5% CO_2. The medium was then removed and replaced by serum-and BSA-free MEM (Thermo Fisher Scientific) for 4 h. Plates were then washed with prewarmed PBS, and freshly prepared gluconeogenesis induction medium (MEM containing 15 mM fructose, 10 mM lactate, 1 mM pyruvate, 5 mM L-alanine, 2 mM L-glutamine, 100 nM dexamethasone, 10 nM glucagon, 5 mM dibutyryl-cAMP, and 300 nM forskolin) was added to each well. A concentration series of each insulin analog was added and the plates incubated for 20 h at 37 °C in a humidified atmosphere containing 5% CO_2. One complete experiment consisted of cells plated on the same day in six 96-well plates that included all test and reference compounds. Each insulin analog concentration was tested in four independent replicates on each plate. The experiment was repeated four times to give five biological replicates for determination of the analog 50% inhibitory concentration (IC_{50}) value.

The cells were harvested and lysed in buffer RLT (QIAGEN, Hilden, Germany). Total ribonucleic acid (RNA) was isolated according to the manufacturer's instructions using an RNeasy 96 Qiacube HT Kit (QIAGEN) that included a genomic DNase digestion step. RNA purity and concentration was tested by random spot checking on a spectrophotometer NanoDrop 8000 (Thermo Fisher Scientific). Reverse transcription of RNA into complementary DNA and subsequent real-time polymerase chain reaction (PCR) was performed in 384-well plates in a ViiA™ 7 PCR thermal cycler and fluorescence plate reader (Thermo Fisher Scientific) using an RNA-to-CT™ 1-Step Kit (Thermo Fisher Scientific) according to the manufacturer's instruction. Reactions contained TaqMan™ Fast Advanced Master Mix (6 µl) and isolated RNA (4 µl). All subsequent steps were followed according to the manufacturer's instructions using Hs00984230_m1 for the reference gene B2M,

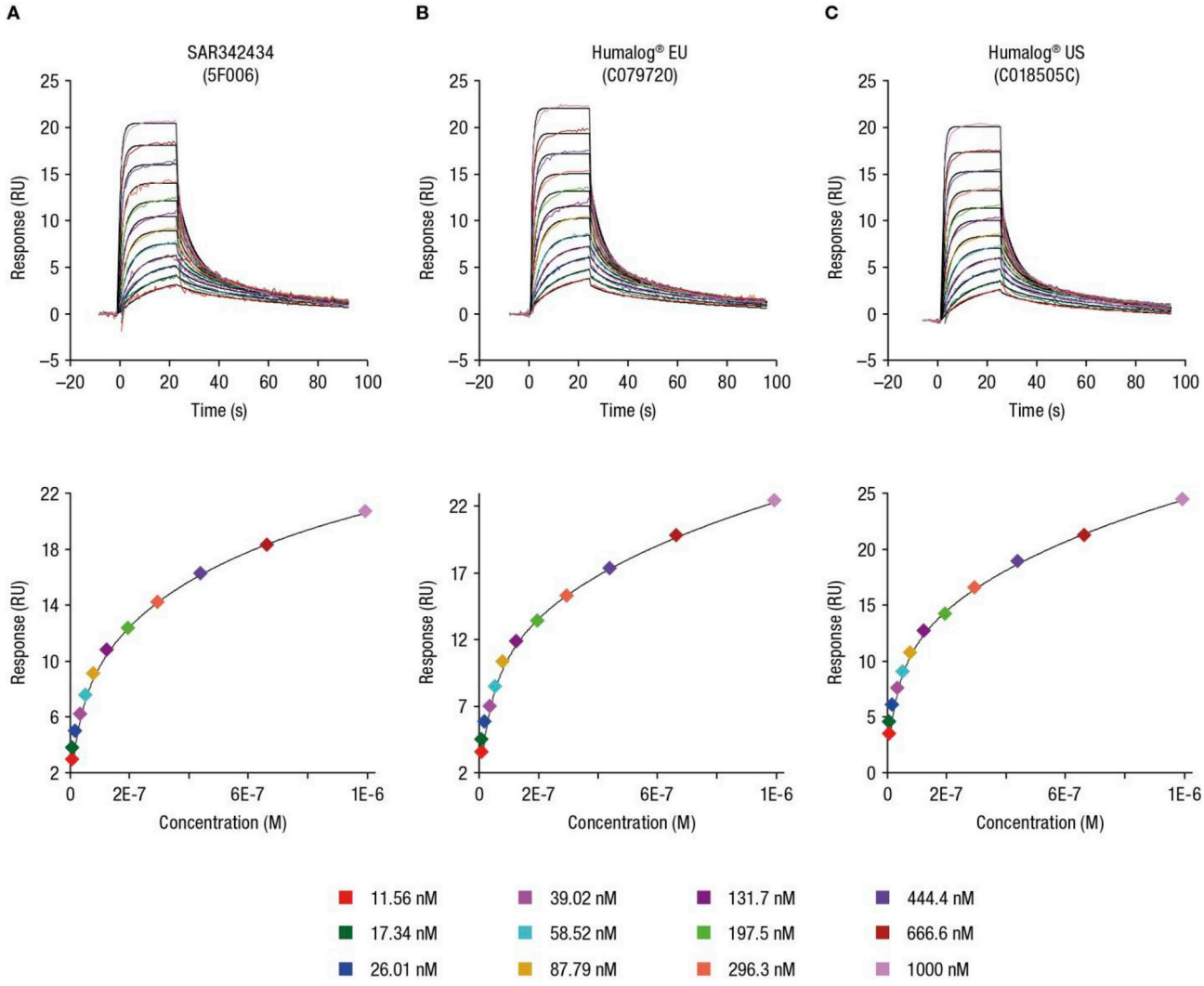

Fig. 1. Representative sensorgram and dose-response plots for the interaction between (A) SAR342434, (B) Humalog® EU, and (C) Humalog® US and the insulin receptor isoform IR-A immobilized to a Biacore chip. RU, relative units; s, second.

and Hs02560787_s1 for the catalytic subunit of glucose-6-phosphatase (G6P) as specific primer assays. For thermal cycling of the PCR reactions, the following temperature–time profile was used: Initial reverse transcription at 48 °C was performed for 15 min followed by denaturation of the reverse transcriptase and activation of polymerase at 95 °C for 15 min. Thereafter, 40 PCR cycles were included consisting of denaturation for 15 s at 95 °C and annealing/extension for 60 s at 60 °C.

The fluorescence–time profiles of G6P gene expression were analyzed using ViiA™ 7 software according to the manufacturer's instructions. Expression levels were determined as cycle threshold (CT) values, which correspond to the number of the PCR amplification cycles necessary to reach a threshold fluorescence signal above background.

2.7. Stimulation of mitogenic activity

Mitogenic activity was determined in MCF-7 cells as described previously for SAOS-2 cells (Sommerfeld et al., 2010). MCF-7 human breast cells, an IGF1R dominant cell line (Liefvendahl and Arnqvist, 2008), were obtained in frozen aliquots from the European Collection of Authenticated Cell Cultures (ECACC, Salisbury, UK). Cells were grown in McCoy's 5A medium (Gibco, Grand Island, NY, USA) supplemented with 10% FCS (PAN-Biotech GmbH) and 2 mM (final) L-glutamine (Sigma-Aldrich, Irvine, UK). Subconfluent cultures (9–15 × 10^6 cells per 225 cm^2 flask) were used to determine the mitogenic activity of the test compounds.

For measuring thymidine incorporation, cells were seeded on 96-well Cytostar-T scintillation microplates (GE Healthcare) and the plates incubated overnight at 37 °C in a humidified atmosphere containing 5% CO_2. The serum-containing medium was removed and replaced by serum-free McCoy's 5A medium supplemented with 0.5% (w/v) BSA, 2 mM L-glutamine, and antibiotics (penicillin 100 units, streptomycin 100 units, amphotericin B 0.25 mg/mL (final; Gibco). The plates were incubated for 4 h at 37 °C in a humidified atmosphere containing 5% CO_2. Following this, three-quarters of the medium was removed and substituted with serum-free medium containing the different insulins at the indicated concentrations, and the plates were incubated at 37 °C in a humidified atmosphere containing 5% CO_2. After 19 h, [2–^{14}C]-thymidine solution (> 50 mmol/L, 3.7 MBq/mL) diluted in serum-free McCoy's 5A medium was added per well to yield a final concentration of 500 nCi/mL, and the plates were incubated for 6 h at 37 °C in a humidified atmosphere containing 5% CO_2. Incorporation of ^{14}C-thymidine was measured in a Wallac 1450 MicroBeta® TriLux scintillation counter (PerkinElmer, Freiburg, Germany). Dose–response curves were obtained by testing 10 different concentrations of the ligands, with every concentration tested by octuplicate samples.

2.8. Statistical analysis

Each batch of SAR342434 and Humalog® EU or US was tested in each assay at least five times using separate plates. The IC_{50} or 50% effective (EC_{50}) concentration value was calculated for each test using a four-parameter logistic model in SAS (V9.2) software (SAS Institute, Cary NC, USA) via internal applications. Biost@t-Binding V3.1 was used for receptor competitive binding with the lower asymptote constrained to the low control level of nonspecific binding. Biost@t-Speed V2.1 LTS was used for receptor autophosphorylation, inhibition of lipolysis, glucose uptake, repression of G6P gene expression, and stimulation of mitogenic activity.

$$Y = Bottom + \frac{Top - Bottom}{(1 + \exp(-slope(\ln X - \ln C50)))}$$

For G6P gene expression, the statistical analysis was based on CT values. CT values were converted to relative normalized expression values by the $2^{-\delta\delta CT}$ Method (Livak and Schmittgen, 2001). Values of normalized expression ($2^{-\delta\delta CT}$) as a function of concentration were used to determine IC_{50} values based on the four-parameter logistic model.

For all IC_{50} or EC_{50} values and all kinetic binding constants for IR-A and IR-B, the weighted geometric means and their respective 95% CIs were calculated first per batch and second per product.

An equivalence approach was used to ascertain similarity between SAR342434 and the Humalog® insulins. The ratios of the weighted geometric mean IC_{50} or EC_{50} values or mean kinetic constants with their 90% CIs were calculated for SAR342434 versus Humalog® EU, SAR342434 versus Humalog® US, and Humalog® EU versus Humalog® US batches using SAS (V9.2). SAR342434 was considered similar to Humalog® US and Humalog® EU if the 90% CI was completely within the predefined acceptance range for each method. The acceptance ranges were defined based on specification limits and the variability of the respective methods.

3. Results

3.1. IR kinetic binding

Fig. 1A–C shows typical sensorgrams and dose–response curves from one experiment for the interaction of SAR342434 (Fig. 1A), Humalog® EU (Fig. 1B), and Humalog® US (Fig. 1C) with human IR-A. The geometric mean (95% CI) kinetic binding constants to human IR-A and IR-B for each insulin analog derived from the sensorgrams are summarized in Table 2. The ka1, kd1, ka2, and kd2 for SAR342434 binding to IR-A were 7.69E+05 1/Ms, 1.55E-01 1/s, 3.52E+06 1/Ms, and 1.90E-02 1/s, respectively. The corresponding values for SAR342434 binding to IR-B were 5.44E+05 1/Ms, 1.30E-01 1/s, 2.18E+06 1/Ms, and 1.51E-02 1/s, respectively. Similar values for each kinetic constant were derived for both Humalog® EU and Humalog® US binding to IR-A and IR-B (Table 2).

3.2. IR-A, IR-B, and IGF1R competitive binding and autophosphorylation

Competitive binding curves of the three insulin analogs to human IR-B, IR-A, and IGF1R, as well as receptor autophosphorylation, are shown in Fig. 2A–F. The IC_{50} values of SAR342434 for competitive binding to human IR-B, IR-A, and IGF1R were 0.63, 0.56, and 28.1 nM respectively; those for Humalog® US and EU were similar (Table 3). The EC_{50} values of SAR342434 for IR-B, IR-A, and IGF1R autophosphorylation were 31.7, 29.7, and 354 nM respectively, and comparable to the EC_{50} values for Humalog® US and EU (Table 3).

3.3. Metabolic and mitogenic activities

Concentration curves of the insulin analogs for metabolic and mitogenic activities are shown in Fig. 3A–D. The IC_{50} value of SAR342434 for inhibition of lipolysis and repression of G6P gene expression, and the EC_{50} value for stimulation of glucose uptake were 0.024, 583, and 12.3 nM, respectively; which were similar to the activities obtained for Humalog® US and EU (Table 3). New in the context of measuring insulin efficacy in cellular metabolic assays, is the gene expression measurement of G6P Upcyte hepatocytes to assess repression of gluconeogenesis. Typically G6P could be highly induced and then repressed approximately 4-fold concentration dependently by insulin Humalogs and SAR342434 biosimilar. Insulin had no significant effect on B2M used at housekeeping gene for normalization (see supplement Fig 1). Regarding cell assays for mitogenecity, the EC_{50} value of SAR342434 for stimulation of MCF-7 cell proliferation was 3.05 nM and comparable to the EC_{50} for Humalog® US and EU (Table 3).

3.4. Similarity between SAR342434 and Humalog® US and EU

Statistical evaluation of the experimental data for SAR342434 and the originator batches, based on specification limits and the variability of the respective methods, demonstrated similarity between SAR342434 and Humalog® US, SAR342434 and Humalog® EU, and Humalog® US and Humalog® EU for all assays, as the 90% CIs of the ratio of means were within the predefined acceptance limits for each assay (Table 4).

4. Discussion

In order to assess any differences in properties between a new insulin biosimilar and the originator insulin, comparative nonclinical investigations that include assays for receptor binding properties as well as biological activity need to be performed before undertaking clinical development (European Medicines Agency, 2015). The current results demonstrate similarity between SAR342434 and Humalog® EU or US in their pharmacologic responses in various *in vitro* assays used for insulin characterization. These included a kinetic binding assay and a third metabolic activity assay, as recommended by the (insulin specific) EMA guidelines (European Medicines Agency, 2015). The

Table 2
Kinetic constants for binding of Humalog® EU and US and SAR342434 to human insulin receptor isoform A or B.

IR Isoform	Parameter	Humalog® (EU)	Humalog® (US)	SAR342434
IR-A	ka1 (1/Ms)	8.00E+05 (7.73E+05–8.28E+05)	7.88E+05 (7.48E+05–8.30E+05)	7.69E+05 (7.37E+05–8.01E+05)
	kd1 (1/s)	1.59E-01 (1.52E-01–1.68E-01)	1.71E-01 (1.61E-01–1.82E-01)	1.55E-01 (1.46E-01–1.64E-01)
	ka2 (1/Ms)	3.50E+06 (3.38E+06–3.63E+06)	3.35E+06 (3.05E+06–3.68E+06)	3.52E+06 (3.37E+06–3.68E+06)
	kd2 (1/s)	1.98E-02 (1.90E-02–2.06E-02)	2.08E-02 (1.97E-02–2.20E-02)	1.90E-02 (1.80E-02–2.00E-02)
IR-B	ka1 (1/Ms)	5.53E+05 (5.32E+05–5.75E+05)	5.58E+05 (5.30E+05–5.87E+05)	5.44E+05 (5.22E+05–5.66E+05)
	kd1 (1/s)	1.32E-01 (1.29E-01–1.36E-01)	1.37E-01 (1.33E-01–1.41E-01)	1.30E-01 (1.25E-01–1.35E-01)
	ka2 (1/Ms)	2.14E+06 (2.08E+06–2.21E+06)	2.11E+06 (1.99E+06–2.24E+06)	2.18E+06 (2.10E+06–2.26E+06)
	kd2 (1/s)	1.57E-02 (1.53E-02–1.61E-02)	1.62E-02 (1.57E-02–1.66E-02)	1.51E-02 (1.47E-02–1.55E-02)

Data are geometric mean (95% CI).

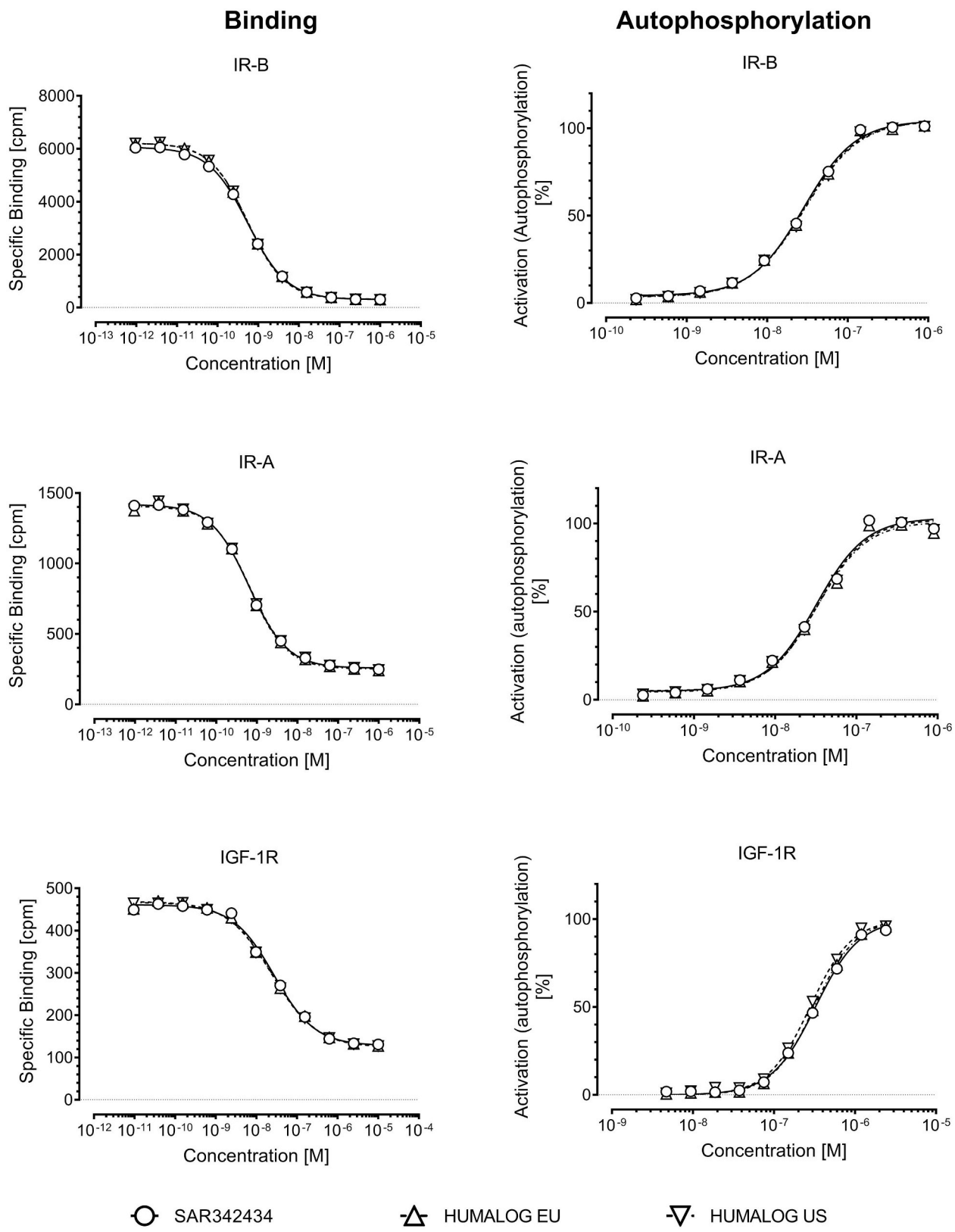

Fig. 2. IR-B, IR-A, and IGF1R competitive binding (A, C, E, respectively) and autophosphorylation (B, D, F, respectively) averaged by the three products, SAR342434 and Humalog® EU and US. Curves with individual batches are available in supplement Fig. 2.

development of a surface plasmon resonance assay for full-length IR is expected to be of importance for future biosimilar studies or in the development of improved insulin analogs.

The equilibrium binding constants of SAR342434 and Humalog® EU or US were similar for both IR-A and IR-B. In addition to equilibrium binding measurements, similarity in on-off kinetics with both human IRs needed to be demonstrated (European Medicines Agency, 2015). Subramanian and colleagues assessed the binding kinetics of insulin to

Table 3
Summary of *in vitro* results for SAR342434 and Humalog® EU or US.

	EC_{50} or IC_{50} (95% CI), nM		
	Humalog® (EU)	Humalog® (US)	SAR342434
IR-B binding	0.54 (0.51–0.57)	0.54 (0.51–0.57)	0.56 (0.53–0.59)
IR-A binding	0.65 (0.59–0.72)	0.65 (0.59–0.73)	0.63 (0.58–0.69)
IR-B autophosphorylation	29.0 (26.8–31.4)	28.0 (25.9–30.1)	29.7 (27.7–31.3)
IR-A autophosphorylation	33.7 (31.5–36.0)	33.8 (31.7–36.2)	31.7 (29.8–33.8)
Lipolysis	0.023 (0.022–0.025)	0.023 (0.022–0.024)	0.024 (0.023–0.026)
Glucose uptake	12.3 (11.3–13.4)	10.8 (10.0–11.7)	12.3 (11.4–13.3)
G6P gene expression	0.536 (0.453–0.635)	0.512 (0.449–0.583)	0.584 (0.487–0.702)
IGF1R binding	25.5 (22.3–29.2)	23.9 (21.1–27.1)	28.1 (24.7–32.0)
IGF1R autophosphorylation	337 (309–369)	295 (274–317)	354 (326–385)
Proliferation	2.79 (2.41–3.24)	2.79 (2.43–3.22)	3.05 (2.66–3.50)

EC_{50}, 50% effective concentration; G6P, glucose-6-phosphatase; IC_{50}, 50% inhibitory concentration.

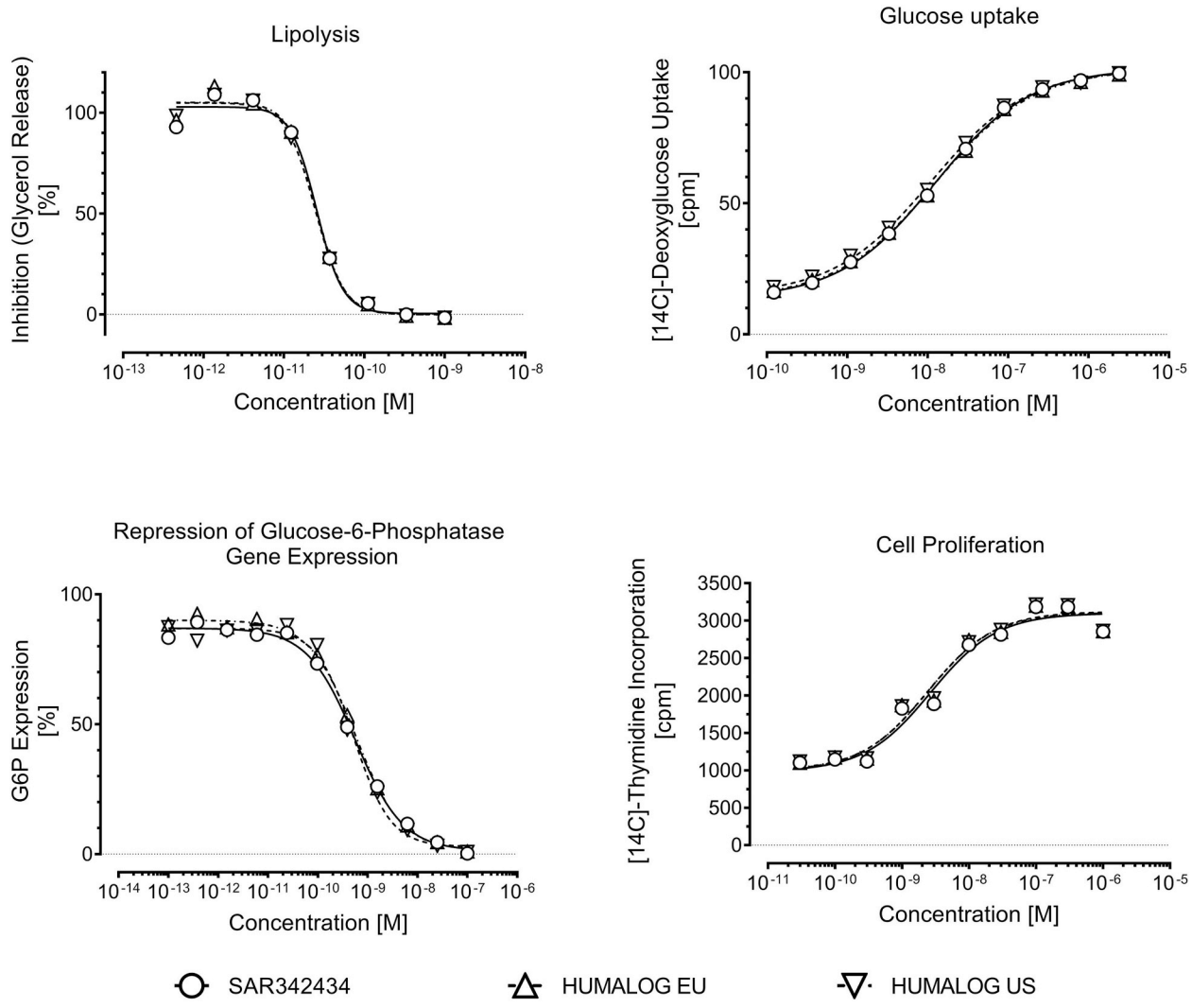

Fig. 3. Concentration-response curves for (A) inhibition of human fat cell lipolysis, (B) stimulation of rat L6 cell glucose uptake, (C) repression of human hepatocyte glucose-6-phosphatase gene expression, and (D) proliferation of MCF-7 breast cancer cells averaged by the three products, SAR342434 and Humalog® EU and US. Curves with individual batches are available in supplement Fig. 3.

an insulin receptor ecto-domain using surface plasmon resonance (Subramanian et al., 2013). Their kinetic binding data could be fitted best by a high-affinity and a second low-affinity binding site in accordance with previous literature. Here we have developed an improved biosensor-based assay, which allows the kinetic binding of insulin to full-length IRs that have been freshly solubilized from cell lines. The solubilized full-length receptors were captured by an antibody that was covalently immobilized to the dextran matrix on the sensor surface. This yielded a stable sensor surface that could be used for the characterization of insulin binding for at least 24 h. The simplest kinetic model that best described the data was a model for two independent binding sites. This is in agreement with the previous work by Subramanian and colleagues. The results revealed that the binding of human insulin or insulin lispro to both human IR isoforms occurs at a

Table 4
Ratio of IC_{50}/EC_{50}: Comparison of SAR342434 with Humalog® EU or US and of Humalog® EU with Humalog® US.

	Acceptance Range	Ratio of IC50 or EC50 (90% CI)		
		Humalog® (EU) vs Humalog® (US)	SAR342434 vs Humalog® (US)	SAR342434 vs. Humalog® (EU)
IR-B binding	[0.80; 1.25]	1.002 (0.945–1.061)	1.033 (0.973–1.098)	1.032 (0.975–1.093)
IR-A binding	[0.75; 1.33]	1.000 (0.906–1.105)	0.993 (0.895–1.102)	0.993 (0.905–1.089)
IR-B autophosphorylation	[0.75; 1.33]	1.038 (0.950–1.134)	0.938 (0.870–1.012)	0.943 (0.840–1.018)
IR-A autophosphorylation	[0.75; 1.33]	0.995 (0.920–1.075)	0.938 (0.870–1.012)	0.943 (0.874–1.018)
Lipolysis	[0.75; 1.33]	1.008 (0.945–1.075)	1.052 (0.989–1.118)	1.043 (0.971–1.121)
Glucose uptake	[0.70; 1.43]	1.147 (1.048–1.257)	1.137 (1.041–1.243)	0.991 (0.904–1.087)
G6P gene expression	[0.70; 1.43]	1.049 (0.884–1.245)	1.142 (0.953–1.368)	1.089 (0.892–1.330)
IGF1R binding	[0.70; 1.43]	1.055 (0.942–1.182)	1.173 (1.052–1.307)	1.111 (0.988–1.251)
IGF1R autophosphorylation	[0.75; 1.33]	1.135 (1.047–1.230)	1.200 (1.169–1.298)	1.057 (0.969–1.154)
Proliferation	[0.70; 1.43]	1.019 (0.879–1.181)	1.089 (0.950–1.250)	1.069 (0.917–1.247)

high-affinity binding site and one low-affinity binding site. The interaction with the high-affinity binding site was characterized by having a higher association rate and a lower dissociation rate than the low-affinity binding site.

The current data do not contradict a more complex binding model, e.g cooperativity between binding sites or an additional induced fit step involving conformational changes of the receptor. Convincing evidences for such an induced fit upon insulin binding has been recently contributed by in two independent cryo electron microscopy derived insulin receptor structures (Scapin et al., 2018; Weis et al 2018). However, further mechanistic kinetic binding studies, beyond the scope to demonstrate similar efficacy of insulin analogs, would be needed to fully elucidate the dynamic interaction mechanism. SAR342434 demonstrated similarity to Humalog® EU or US with respect to the association and dissociation rate constants for both IR isoforms.

In addition to comparisons of both kinetic and equilibrium binding, the EMA recommends comparison of biological activity at two levels: receptor autophosphorylation and metabolic activity. SAR342434 also demonstrated similarity to Humalog® EU or US with respect to IR autophosphorylation for both receptor subtypes. In accordance with the EMA guidelines (European Medicines Agency, 2015), three *in vitro* metabolic assays were employed, each one representative of an important site of action for insulin: inhibition of lipolysis in *in vitro* differentiated human adipocytes, stimulation of glucose uptake in L6 muscle cells, and repression of G6P gene expression in human hepatocytes.

As a new third metabolic activity assay, we introduced here the use of human Upcyte hepatocytes to compare insulin biosimilars and analogs on efficacy of repression of gluconeogenesis genes. Upcyte hepatocytes are derived from primary human hepatocytes transduced with viral particles containing proliferation-inducing genes (Burkard et al., 2012). These cells were initially established to assess hepatic drug metabolism and toxicity. Recently, it could be demonstrated that upon differentiation, metabolically functional, polarized hepatocytes are formed with functional bile canaliculi (Levy et al., 2015). The present paper describes for the first time that insulins display a high potency in repressing gluconeogenesis in these modified hepatocytes, one of a key metabolic efficacies of insulins. SAR342434 demonstrated similarity with Humalog® EU or US in each of the selected cellular metabolic assays.

Insulin analogs may have mitogenic activity, so the EMA has indicated that comparative IGF1R binding and an assay for functional activity can be included to cover this potential risk. In the IGF1R binding and autophosphorylation assays, the EC50 seems to be slightly higher for SAR342434 than Humalog US but not when compared to Humalog EU. The statistical comparison of SAR342434 with its comparators Humalog EU and Humalog US is based on an equivalence approach, which covers that systematic differences between the products are not confounded with the random variability of the experimental method. To ensure this, acceptance ranges for equivalence between products are defined based on the variations of the individual test parameters. These variations then only contain the method variability without any between-batch or between-product variability, consequently the acceptance ranges ensure that any additional systematic deviation or between-product variability will be detected. Apparent differences between two products which are within these ranges, like in the IGF1R binding assay, cannot be distinguished from method variability. We therefore consider this as a purely random effect. In accordance, in the MCF-7 cell proliferation assay the SAR342434 mean values lie well within the 90% confidence intervals for both Humalog sources without any apparent different mitogenic activity.

The similarity of SAR342434 to Humalog® EU or US demonstrated in our nonclinical studies formed the basis for the clinical development program where SAR342434 was found to have similarity with Humalog® EU or US with regard to pharmacokinetics/pharmacodynamics (Kapitza et al., 2017), as well as in phase III clinical trials in patients with type 1 or type 2 diabetes mellitus (Garg et al., 2017; Derwahl et al., 2018).

In conclusion, based on side-by-side biological similarity assessment in a panel of *in vitro* assays, insulin lispro as SAR342434 solution, Humalog® EU, and Humalog® US can be considered as similar.

Funding

The studies were funded by Sanofi-Aventis Deutschland GmbH.

Authorship contributions

Participated in research design: M.K., P.W., T.G., J.D., and N.T.
Conducted experiments: M.K., P.W., T.G., J.D., M.K-M., and N.T.
Performed data analysis: M.K., P.W., T.G., J.D., B.N., and N.T.
Wrote or contributed to the writing of the manuscript: M.K., P.W., T.G., J.D., M.K-M., B.N., and N.T.

Conflicts of interest

M.K., P.W., J.D., B.N., and N.T. are employees of Sanofi-Aventis Deutschland GmbH. T.G. is an employee of Beactica AB. M.K-M. is a former employee of Beactica AB.

Declaration of competing interest

The authors declare that they have no known competing financial interests or personal relationships that could have appeared to influence the work reported in this paper.

Acknowledgments

The study was funded by Sanofi-Aventis Deutschland GmbH. Editorial support was provided by Caroline Cook and Tom Claus

(Parexel International NJ, USA) and funded by Sanofi US. The authors would like to thank members from the *in vitro* laboratories involved at Sanofi for excellent technical support. We thank Adrienne Pall for the support in graphing data.

Appendix A. Supplementary data

Supplementary data to this article can be found online at https://doi.org/10.1016/j.yrtph.2019.104497.

References

American Diabetes Association, 2018. Standards of medical care in diabetes-2018. Diabetes Care 41 (Suppl. 1), S1–S159.

Baus, D., Heermeier, K., De Hoop, M., Metz-Weidmann, C., Gassenhuber, J., Dittrich, W., et al., 2008. Identification of a novel AS160 splice variant that regulates GLUT4 translocation and glucose-uptake in rat muscle cells. Cell. Signal. 20 (12), 2237–2246. https://doi.org/10.1016/j.cellsig.2008.08.010.

Baus, D., Yan, Y., Li, Z., Garyantes, T., de Hoop, M., Tennagels, N., 2010. A robust assay measuring GLUT4 translocation in rat myoblasts overexpressing GLUT4-myc and AS160_v2. Anal. Biochem. 397 (2), 233–240. https://doi.org/10.1016/j.ab.2009.10.036.

Burkard, A., Dahn, C., Heinz, S., Zutavern, A., Sonntag-Buck, V., Maltman, D., et al., 2012. Generation of proliferating human hepatocytes using Upcyte(R) technology: characterisation and applications in induction and cytotoxicity assays. Xenobiotica 42 (10), 939–956. https://doi.org/10.3109/00498254.2012.675093.

Derwahl, K.M., Bailey, T.S., Wernicke-Panten, K., Ping, L., Pierre, S., 2018. Efficacy and safety of biosimilar SAR342434 insulin lispro in adults with type 2 diabetes, also using insulin glargine: SORELLA 2 study. Diabetes Technol. Ther. 20 (1), 49–58. https://doi.org/10.1089/dia.2017.0281.

European Medicines Agency, 2012. Guideline on clinical investigation of medicinal products in the treatment or prevention of diabetes mellitus. http://www.ema.europa.eu/docs/en_GB/document_library/Scientific_guideline/2012/06/WC500129256.pdf, Accessed date: 30 December 2018.

European Medicines Agency, 2014. Guideline on similar biological medicinal products. Committee for Medicinal Products for Human Use (CHMP). http://www.ema.europa.eu/docs/en_GB/document_library/Scientific_guideline/2014/10/WC500176768.pdf, Accessed date: 30 December 2018.

European Medicines Agency, 2015. Guideline on nonclinical and clinical development of similar biological medicinal products containing recombinant human insulin and insulin analogues. http://www.ema.europa.eu/docs/en_GB/document_library/Scientific_guideline/2015/03/WC500184161.pdf, Accessed date: 30 December 2018.

Garg, S.K., Wernicke-Panten, K., Rojeski, M., Pierre, S., Kirchhein, Y., Jedynasty, K., 2017. Efficacy and safety of biosimilar SAR342434 insulin lispro in adults with type 1 diabetes also using insulin glargine-SORELLA 1 study. Diabetes Technol. Ther. 19 (9), 516–526. https://doi.org/10.1089/dia.2017.0117.

Kapitza, C., Nowotny, I., Lehmann, A., Bergmann, K., Rotthaeuser, B., Nosek, L., et al., 2017. Similar pharmacokinetics and pharmacodynamics of rapid-acting insulin lispro products SAR342434 and US- and EU-approved Humalog in subjects with type 1 diabetes. Diabetes Obes. Metab. 19 (5), 622–627. https://doi.org/10.1111/dom.12856.

Levy, G., Bomze, D., Heinz, S., Ramachandran, S.D., Noerenberg, A., Cohen, M., Shibolet, O., Sklan, E., et al., 2015. Long-term culture and expansion of primary human hepatocytes. Nat. Biotechnol. 33 (12), 1264–1271. https://doi.org/10.1038/nbt.3377. 2015 Dec.

Liefvendahl, E., Arnqvist, H.J., 2008. Mitogenic effect of the insulin analogue glargine in malignant cells in comparison with insulin and IGF-I. Horm. Metab. Res. 40 (6), 369–374. https://doi.org/10.1055/s-2008-1062739.

Livak, K.J., Schmittgen, T.D., 2001. Analysis of relative gene expression data using real-time quantitative PCR and the 2(-Delta Delta C(T)) Method. Methods 25 (4), 402–408. https://doi.org/10.1006/meth.2001.1262.

Rissler, K., Engelmann, P., 1996. Labeling of insulin with non-radioactive 127I and application to incorporation of radioactive 125I for use in receptor-binding experiments by high-performance liquid chromatography. J. Chromatogr. B Biomed. Appl. 679 (1–2), 21–29.

Scapin, G., Dandey, V.P., Zhang, Z., Prosise, W., Hruza, A., Kelly, T., Mayhood, T., Strickland, C., Potter, C.S., Carragher, B., 2018. Structure of the insulin receptor-insulin complex by single-particle cryo-EM analysis. Nature 556 (7699), 122–125. https://doi.org/10.1038/nature26153.

Sommerfeld, M.R., Muller, G., Tschank, G., Seipke, G., Habermann, P., Kurrle, R., et al., 2010. In vitro metabolic and mitogenic signaling of insulin glargine and its metabolites. PLoS One 5 (3), e9540. https://doi.org/10.1371/journal.pone.0009540.

Subramanian, K., Fee, C.J., Fredericks, R., Stubbs, R.S., Hayes, M.T., 2013. Insulin receptor-insulin interaction kinetics using multiplex surface plasmon resonance. J. Mol. Recognit. 26 (12), 643–652. https://doi.org/10.1002/jmr.2307.

US Food and Drug Administration and Center for Drug Evaluation and Research (CDER), 1999. Guidance for industry. Applications covered by Section 505(b)(2). Draft guidance. https://www.fda.gov/downloads/Drugs/Guidances/ucm079345.pdf, Accessed date: 30 May 2018.

US Food and Drug Administration and Center for Drug Evaluation and Research (CDER), 2008. Guidance for industry. Diabetes mellitus: developing drugs and therapeutic biologics for treatment and prevention. Draft guidance. https://www.fda.gov/downloads/Drugs/.../Guidances/ucm071624.pdf, Accessed date: 30 May 2018.

Voss, M.D., Beha, A., Tennagels, N., Tschank, G., Herling, A.W., Quint, M., et al., 2005. Gene expression profiling in skeletal muscle of Zucker diabetic fatty rats: implications for a role of stearoyl-CoA desaturase 1 in insulin resistance. Diabetologia 48 (12), 2622–2630. https://doi.org/10.1007/s00125-005-0025-2.

Weis, F., Menting, J.G., Margetts, M.B., Chan, S.J., Xu, Y., Tennagels, N., Wohlfart, P., Langer, T., Müller, C.W., Dreyer, M.K., Lawrence, M.C., 2018. The signalling conformation of the insulin receptor ectodomain. Nat. Commun. 9 (1), 4420. https://doi.org/10.1038/s41467-018-06826-6. Oct 24.

Werner, U., Korn, M., Schmidt, R., Wendrich, T.M., Tennagels, N., 2014. Metabolic effect and receptor signalling profile of a non-metabolisable insulin glargine analogue. Arch. Physiol. Biochem. 120 (4), 158–165. https://doi.org/10.3109/13813455.2014.950589.